Carbohydrate Polymers 117 (2015) 644–649

Contents lists available at ScienceDirect

Carbohydrate Polymers

journal homepage: www.elsevier.com/locate/carbpol

Pyrolytic and kinetic characteristics of *Platycodon Grandiflorum* peel and its cellulose extract

Hong-Wei Qiu[a,1], Quan-Cheng Zhou[b,c,*,1], Jie Geng[c]

[a] Qingdao Agricultural University, Zibo 255049, China
[b] State Key Laboratory of Pharmaceutical Biotechnology, Nanjing University, Nanjing 210032, China
[c] School of Agricultural Engineering and Food Science, Shandong University of Technology, Zibo 255049, China

ARTICLE INFO

Article history:
Received 25 April 2014
Received in revised form 4 September 2014
Accepted 6 September 2014
Available online 28 September 2014

Keywords:
Platycodon grandiflorum peel
Cellulose
Pyrolysis
Kinetics

ABSTRACT

The pyrolytic and kinetic characteristics of a biomass waste material, namely *Platycodon grandiflorum A. DC* (*P. G.*) peel and its cellulose extract were studied at heating rates of 10, 30 and 50 °C/min under a nitrogen flow atmosphere. The most probable mechanism function and activation energy pre-exponential factors were calculated by using the Popescu, FWO and KAS methods. The three stages appeared during pyrolysis include: moisture evaporation, primary devolatilization and residual decomposition. Significant differences in the average activation energy, thermal stability, final residuals and reaction rates of the *P. G.* peel and its cellulose extract were observed. Stage II of the *P. G.* peel and its cellulose extract could be described by the function Avrami–Erofeev $[-\ln(1-\alpha)]^3$ and the function chemical reaction $(1-\alpha)^{-0.5}$, respectively. The average activation energy of *P. G.* peel and its cellulose extract were 157 and 196 kJ/mol, respectively. Kinetic compensation effects of the pre-exponential factors and activation energy were also observed.

1. Introduction

Platycodon grandiflorum A. DC (*P. G.*) has been used as either a food material or a traditional oriental medicine in China and Korea, such as for treating cough, phlegm, sore throat, hyperlipidemia, hypertension and diabetes. As a sustainable and clean bio-energy resource, *P. G.* has great potential for its high carbohydrate content (about 50% of the total weight) and the major carbohydrate is oligosaccharide that is utilized to produce ethanol (He et al., 2005; Zhou, 2011). In addition, the plant area of *P. G.* is about 13 million m^2 and the amount of wasted *P. G.* peels is 200 t (http://www.cu-market.com.cn/hgjj/2010-8-31/14253045.html). Huge amounts of *P. G.* peels are discarded as useless residues, which caused not only the environmental pollution but also a waste of bio-resource.

Bio-oil and chemical products can be extracted from the residues of pyrolysis (Cornelia, Carmen, Popescu, Brebu, & Stefan, 2011). But the carbonhydrate composition and form have a strong effect on pyrolytic reaction and behavior (Korkut, 2011; Cai & Bi, 2009). So both the development of the pyrolytic process and pyrolytic reactor design require complete elucidation of the pyrolytic mechanism.

Cellulose is the most abundant polymer on the earth (Korkut, 2011; Cai & Bi, 2009). Understanding the cellulose thermal degradation is of great importance in a vast array of areas such as generation of energy from biomass and the improvement in flame retardants of cellulosic fibers (Cai & Bi, 2009; He, Yi, & Sun, 2002; Li et al., 2010; Luis & Noureddine, 2010; Matheus, Juliane, Vinícios, Mara, & Ademir, 2010). Although extensive research focusing on cellulose pyrolysis, especially research on the effects of chemicals and different pretreatment on cellulose pyrolysis have been conducted (Dorez, Ferry, Sonnier, Taguet, & Lopez-Cuesta, 2014; Lédé, 2012; Matsuoka, Kawamoto, & Saka, 2014; Shaik, Sharratt, & Tan, 2013; Wei et al., 2014), it is not yet fully understood on pyrolytic process and kinetics model of *P. G.* peel and cellulose extract. Besides, it is not well introduced on the application of differential thermal and thermo-gravimetric analyzes to cellulose and its derivatives.

Thermogravimetric (TG) analysis is a widely used technique in this area (Li et al., 2010; Matheus et al., 2010). It is useful for the thermal characterization of both inorganic and organic materials, including polymers (such as cellulose) (Luis & Noureddine, 2010; Raveendran, Ganesh, & Khilar, 1996). It provides quantitative results regarding the loss of mass as a function of increasing temperature or time. Moreover, TG provides basic information on

* Corresponding author at: Zhangzhou Road 12th, Zibo 255049, Shandong, China. Tel.: +86 0533 2786382; fax: +86 0533 2786382.
E-mail address: zhouquancheng@126.com (Q.-C. Zhou).
[1] Both authors contributed equally to this work.

http://dx.doi.org/10.1016/j.carbpol.2014.09.034
0144-8617/

the thermal properties of the material and its composition. The first derivative thermogravimetry (DTG) can be used to investigate the differences among TG curves (Matheus et al., 2010).

In conclusion, kinetics and thermal decomposition mechanisms for the pyrolysis of hemicelluloses, cellulose and lignin in different biomass materials have been extensively studied (Korkut, 2011; Cai & Bi, 2009; He et al., 2002; Li et al., 2010; Luis & Noureddine, 2010; Matheus et al., 2010; Raveendran et al., 1996). But pyrolytic characteristics study on *P. G.* peel and its cellulose extract have not been reported in the literature. Therefore, in order to efficiently utilize *P. G.* peel and its residues, the pyrolytic and kinetic characteristics of *P. G.* peel and its cellulose extract were evaluated at different heating rates using TG–DTG in the present study. The kinetic parameters of decomposition were then obtained and the pyrolytic mechanism was illustrated.

2. Materials and methods

2.1. Sample preparation

P. G. peel and cellulose extract were collected in April 2012 from Shanxi Yanglin Jindao Sprout Company. They were then Cellulose extracted from *P. G.* peel powder by chlorination and alkaline extraction method. The dried *P. G.* peels were pulverized in a plant disintegrator, screened using 120-mesh sieve and dried at 105 °C in hot air oven for 8 h. The screened sample was then delignified with 7 kg m^3 sodium chlorite solution adjusted to a pH 4–4.2 by the addition of acetic acid sodium acetate buffer, at 100 °C for 2 h using a fiber to liquor ratio of 1:50. After being filtered and extensively washed with 2% sodium bisulphate, distilled water and ethanol, the residue (holocellulose or delignified cellulose) was dried at 105 °C in an oven until constant weight. The crude holocellulose was then treated with 175 g/L NaOH solution at 20 °C for 45 min, filtered, washed with 10% acetic acid and then with distilled water. Finally, extracted cellulose was dried at 105 °C in an oven until constant weight. The extracted crude cellulose was treated with volume concentrations of 0.8 m^3/m^3 acetic acid and 0.7 m^3/m^3 nitric acid in 10:1 ratio at 120 °C for 15 min. After being cooled, it was then washed sequentially with 0.95 m^3/m^3 ethanol and distilled water to remove excess of acid mixture. Finally, the purified cellulose was dried at 105 °C in an oven until constant weight. The above procedure of cellulose extraction was adopted from Maheswari, Obi Reddy, Muzenda, Guduri, and Varada (2012).

2.2. Pyrolysis

Pyrolytic characteristics were determined using a thermal analyzer (TG/DSC STA449C-QMS403C, Netzsch Instruments Co. Ltd., Germany). Samples were placed into aluminum oxide crucibles with lids on a high-accuracy DSC-cp sample holder, after which they were heated from ambient temperature to 800 °C at rates of 10, 30 and 50 °C/min in a furnace under a nitrogen flow of 80 mL/min. The sample mass used in each experiment was 10 mg. Weight losses and calorific changes in response to temperature were recorded and used to plot TG analysis and DTG curves. All experiments were conducted in duplicate. All the plots were generated and the lines were fitted using Origin 7.5 software (Origin Lab Corporation).

2.3. Pyrolytic analysis kinetics parameters and mechanism

Through FWO (Li et al., 2010), KAS (Hu et al., 2008) and Popescu methods (Li, Chen, Zhang, Ye, & Xing, 2011), the parameters of thermal analysis kinetics are solved and the kinetic mechanism functions of Popescu (skipping the functional equation and results) were analyzed (Hu et al., 2008). FWO equation:

$$\ln\beta = \ln\left(\frac{0.0048}{R}\frac{A}{G}\frac{E}{(\alpha)}\right) - 1.0516\ \frac{E}{RT} \tag{1}$$

$$\ln\left(\frac{\beta}{T^2}\right) = \ln\left(\frac{A}{E}\frac{R}{G(\alpha)}\right) - \frac{E}{RT} \tag{2}$$

KAS equation:

$$\ln\left(\frac{\beta}{T_n - T_m}\right) = \ln\left[\frac{A}{G(\alpha)}\right] - \frac{E}{RT_\xi} \tag{3}$$

Popescu equation:

$$T\xi = \frac{T_m + T_n}{2} \tag{4}$$

in which: β—heating rate, $\beta = (dT/dt)$, °C/min; E—activation energy, J/mol; A—pre-exponential factor; in chemical kinetics, the pre-exponential factor or A factor is the pre-exponential constant in the Arrhenius equation, an empirical relationship between temperature and rate coefficient.R—molar gas constant, 8.314; $G(\alpha)$—integral mechanism function; T, T_n, T_m, T_ξ—temperature at time of n, m, ξ min.

Table 1
Weight loss and average reaction rate at different stages.

Stage		*P. G.* peel			Cellulose extract		
		Heating rate (°C/min)			Heating rate (°C/min)		
		10	30	50	10	30	50
I	Weight loss (%)	7.76	6.19	6.46	3.36	3.42	2.94
	Time (min)	10.9	4.96	3.45	7.78	3.61	2.53
	Average rate (°C)	0.71	1.25	1.87	0.43	0.95	1.16
II	Weight loss (%)	42.5	43.4	45.0	29.6	30.3	31.8
	Time (min)	23.9	5.62	7.72	16.23	5.32	6.40
	Average rate (°C)	1.78	7.72	5.83	1.82	5.69	4.96
	Temperature range	124–369	143–383	150–400	92–259	102–271	103–283
	Temperature with maximum weight loss	311	326	334	152	164	168
III	Weight loss (%)	18.6	18.5	17.1	33.0	33.0	31.4
	Time (min)	42.37	13.02	7.34	23.7	6.60	3.49
	Average rate (°C)	0.44	1.42	2.33	1.40	4.99	9.00
	Final weight at 800 °C (%)	31.1	32.0	31.5	34.0	33.4	33.9

Reaction conditions: thermal analyzer: TG/DSC STA449, NETZSCH Instruments Co. Ltd., Germany. Temperature range: from ambient temperature to 800 °C. Heating rate: 10, 30 and 50 °C/min under a nitrogen atmosphere of 30 mL/min. Sample mass: 10 mg.

2.4. Statistical analysis

Results are expressed as the mean. Data were analyzed by ANOVA with Origin 7.5 software (Origin Lab Corporation) statistical software. The differences between the means were analyzed by Student-*t* test for multiple comparisons. The level of significance was considered at $p < 0.05$.

3. Results and discussion

3.1. Characteristics of the thermal degradation process

During Stage I, the weight losses of the two samples (Table 1) are primarily due to the loss of moisture absorbed by natural fibers. That is, cellular water and the external water bound by surface tension are lost. Stage II involves devolatilization and is referred as active pyrolysis zone since mass loss rate is high and the main pyrolytic process occurs during this stage. With TG curves of cellulose and lignin standards, the 2nd and 3rd steps were corresponding to the thermal degradation of cellulose and lignin of the wood sample. In this stage, various volatile components are gradually released, resulting in a large weight loss and formation of the main pyrolytic products. However, the beginning temperatures of decomposition of *P. G.* peel at each heating rate are higher than those of cellulose extract at the same heating rate, because pyrolysis of *P. G.* peel is a kind of natural fiber mainly composed of cellulose, hemicelluloses, xylan and lignin. Xylan starts to degrade earlier and decomposes in the range 220–350 °C. The low thermal stability of xylan is assumed to be due to a lower degree of polymerization compared to cellulose and lignin (Wang, Ru, Lin, & Luo, 2013). The small shoulder at around 250 °C shows the presence of a minor reaction, and is followed by a major reaction

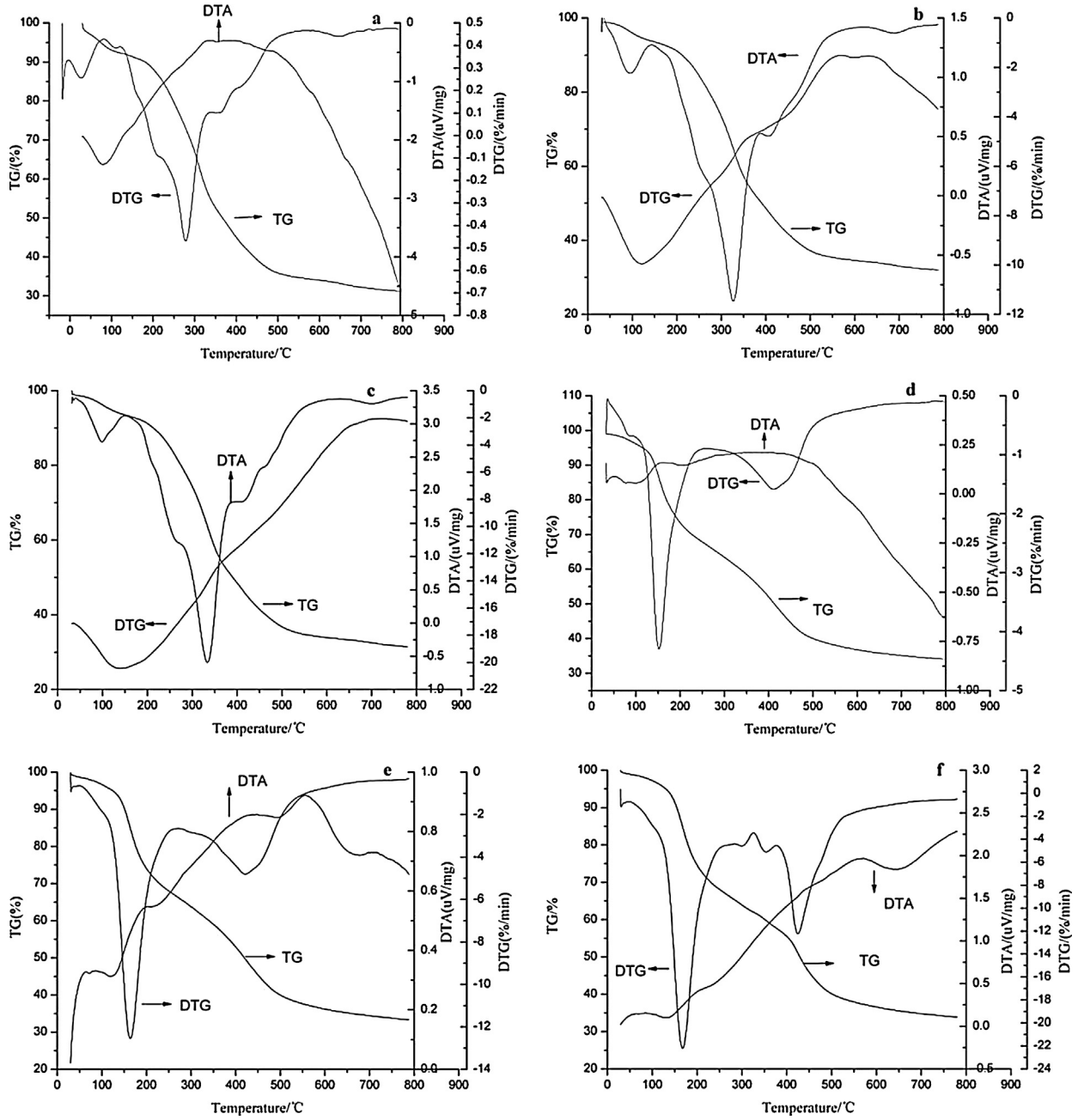

Fig. 1. TG–DTG–DTA curves of samples at different heating rate under a nitrogen atmosphere of 30 mL/min. (a)–(c) 10, 30 and 50 °C/min of *P. G.* peel; (d)–(f) 10, 30 and 50 °C/min of cellulose extract.

Table 2
Pyrolysis characteristic parameters of *P. G.* peel and Cellulose extract.

Sample	Heating rate (°C/min)	T_1 (°C)	T_2 (°C)	T_{max} (°C)	$(d\alpha/dt)_{max}$ (%/min)	I ($\times 10^{-5}$)
P. G. peel	10	124	311	369	3.7	3.11
	30	143	327	388	11.5	9.44
	50	150	334	400	20.0	16.2
Cellulose extract	10	92	259	151	4.3	6.06
	30	102	271	164	12.5	17.0
	50	103	283	168	22.2	28.0

which occurs as an intensive peak at around 311–334 °C to *P. G.* peel. This decomposition stage is due to the degradation of cellulosic and hemicellulose substances (Brebu & Vasile, 2010; Hajaligol, Waymack, & Kellogg, 2001). The decomposition of hemicellulose occurs around 250–370 °C. The degradation of the α—cellulose by depolymerization is between 340 and 370 °C. The degradation of lignin occurs over a wide range of temperature (200–500 °C) (Dorez et al., 2014). During Stage III, the residue slowly decomposes, resulting in the formation of a loose porous residue. Therefore, the beginning temperature of decomposition is lower than halobios biomass such as microalgae, macroalgae and seaweed (Matheus et al., 2010; Li et al., 2011). Because peel and cellulose are composed of many high polymerization polysaccharides, and compared with macroalgae, there is less inorganic salt which has a catalytic effect on decomposition (Rupérez, 2002; Jones, Darvella, Bridgemana, Pourkashaniana, & Wliamsa, 2007). The amount of final residue of cellulose extract at 800 °C was all more than those of *P. G.* peel. In addition, the instantaneous maximum reaction rate is fluctuated among the two samples in different stage and at different heating rate. The results suggest that larger quantities of holocellulose and lignin associated with lower extractive contents give the wood greater thermal stability (Matheus et al., 2010). Degradation of non-cellulose: This stage (after degradation temperature) is attributed to the degradation of non-cellulosic substances such as lignin (Van de Velde & Baetens, 2001; Wong, Shanks, & Hodzic, 2004). Lignin decomposes slower than the cellulose and hemicelluloses over a broader temperature ranging from 200 to 500 °C (Brebu & Vasile, 2010; Hajaligol et al., 2001).

The heating rate had a significant effect on pyrolysis of the two samples. Specifically, as the heating rate increases, the initial pyrolytic temperature, the average reaction rate, the temperature at which maximum weight loss and pyrolytic temperature range occur all increase (Table 1). This phenomenon is similar to a previous description of various biomass feedstocks (Jeguirim & Trouvé, 2009). The increased heating rate provides higher thermal energy to facilitate better heat transfer between the surroundings and the inside of the samples (Park, Kim, Kim, & Park, 2009). The results indicate the following thermal stability order: cellulose extract >*P. G.* peel. The parameters differences in the three stages of pyrolysis help the efficient utilization of different compositions in *P. G.* peel and cellulose extract. Take *P. G.* peel as an example, the heating rate 10 °C/min in stage I is helpful to produce more water loss, which supplies the drier material for the latter stage and benefits for better pyrolytic product of the latter stage. In stage II and III, the heating rate 30 °C/min is best for cellulose and lignin to be decomposed and efficiently get better product with more weight. On the contrary, the heating rate 30 °C/min is optimal for cellulose extract to be efficiently pyrolyzed.

The DTA curves of the samples are shown in Fig. 1. DTA curves are different for *P. G.* peel and cellulose extract. To *P. G.* peel, an endothermic peak occurred at the initial pyrolytic stage, which corresponds with moisture evaporation and accords with the theory that drying process needs endothermic. However, an endothermic peak occurs after a small exothermic effect during cellulose extract pyrolytic reaction. An exothermic effect appears during Stage II as the temperature increases, with exothermic peaks being observed after the corresponding maximum weight loss point. As the temperature continues to rise, there are differences among the DTA curves produced by using different heating rates. As the heating rate increases, the exothermic effect is heightened and the peak area increases. This may be caused by increases in the sample quantity per unit time with the increasing heating rate. The result indicates that the main pyrolysis process in these samples is exothermic. The exothermic effect is due to the charring process of cellulose extract.

Similar results come out with corn stalk and wheat straw by He et al. (2002). In contrast, there is a notable endothermic peak on the DTA curve of *P. G.* peel, which precedes the maximum exothermic peak. The pyrolysis of cellulose extract has no clear endothermic effect because the decomposition process needs very low energy. The same results are obtained with macroalgae because the inorganic salts in macroalgae promote charring and exothermic effects (Park et al., 2009).

3.2. Kinetic analysis of the pyrolysis process

Table 2 shows that I of the two samples increased with heating rate growth, which means that when the heating rate is higher, it will enhance pyrolytic reaction of the two samples. Furthermore, the pyrolytic reaction of cellulose extract occurs more easily than that of *P. G.* peel, which corresponds to the results in Table 1 and accords with the results in literatures (Dorez et al., 2014; Wang et al., 2013). *P. G.* peel has other fibers than cellulose, such as xylan, which has a higher pyrolytic temperature. This stage is due to the vaporization of the moisture in the fibers. Chemically treated fibers

Table 3
The linear fitting results of kinetic mechanism function.

Sample	Function.	Temperature (°C)	r	SD
P. G. peel	Avrami–Erofeev function $n = 3$	160	0.9964	0.0000
		210	0.9993	0.0001
		260	0.9996	0.0020
		310	0.9996	0.0207
		360	0.9992	2.0365
Cellulose extract	Chemical reaction	105	1.0000	6.85E − 05
		140	1.0000	1.01E − 05
		175	0.9746	0.0368
		210	0.9678	0.0746
		245	0.9798	0.2561

Table 4
The kinetic parameter obtained by FWO and KAS at different conversion rate of *P. G.* peel and Cellulose extract.

	α	FWO			KAS				Popescu		
		E (kJ/mol)	R	$\ln A$ ($\min^{-1}$)	E (kJ/mol)	R	$\ln A$ ($\min^{-1}$)	α	E (kJ/mol)	R	$\ln A$ ($\min^{-1}$)
P. G. peel	0.1	148	0.9982	30.4	147	0.9981	30.3	0.2–0.1	154	0.9980	34.8
	0.2	155	0.9985	32.1	154	0.9983	32.0	0.3–0.2	146	0.9950	31.5
	0.3	149	0.9963	30.6	147	0.9959	30.3	0.4–0.3	62	0.9284	12.1
	0.4	105	0.9905	21.1	101	0.9888	20.0	0.5–0.4	174	0.9995	35.5
	0.5	159	0.9990	32.5	157	0.9989	32.2	0.6–0.5	188	0.9985	37.6
	0.6	176	0.9989	36.3	176	0.9987	36.1	0.7–0.6	179	0.9995	35.3
	0.7	178	0.9998	36.7	178	0.9998	36.5	0.8–0.7	172	0.9995	33.4
	0.8	176	0.9998	36.3	175	0.9998	36.0	0.9–0.8	177	0.9995	33.5
	0.9	178	1.0000	36.6	176	1.0000	36.3				
Average		158			157				157		
Cell ulose extr act	0.1	186	0.9903	56.4	189.1	0.9896	57.07	0.2–0.1	200	0.9986	55.9
	0.2	196	0.9984	57.7	199.6	0.9983	58.39	0.3–0.2	175	0.9986	48.2
	0.3	181	0.9988	52.0	182.8	0.9987	52.52	0.4–0.3	184	1.0000	49.9
	0.4	181	0.9998	51.4	183.3	0.9998	51.86	0.5–0.4	185	0.9997	49.5
	0.5	182	0.9999	50.8	184.0	0.9999	51.24	0.6–0.5	220	0.9950	58.1
	0.6	207	0.9967	56.6	209.7	0.9965	57.26	0.7–0.6	224	0.9916	58.0
	0.7	219	0.9921	58.3	222.2	0.9916	59.09	0.8–0.7	206	0.9895	51.6
	0.8	203	0.9909	52.5	205.8	0.9902	52.99	0.9–0.8	179	0.9744	43.3
	0.9	176	0.9779	43.4	176.4	0.9758	43.54				
Average		192			195				196		

had less moisture, which is a desired trait for fiber reinforced polymer composites (Mohammad et al., 2014; Hossain, Dewan, Hosur, & Jeelani, 2011).

Different conversion rates at different heating rates and temperatures were chosen to determine the pyrolysis mechanism function. These temperatures should be applied during Stage II (Table 3). The mechanism was analyzed according to the Popescu method (Hu et al., 2008) (Table 3). Table 3 shows that function Avrami–Erofeev $[-\ln(1-\alpha)]^3$ is the best for *P. G.* peel, which means that random nucleation and then growth were predominant during the main pyrolysis of *P. G.* peel. Table 3 also shows that function chemical reaction $(1-\alpha)^{-0.5}$ is the best for cellulose extract, which means that chemical reaction was predominant during the main pyrolysis of cellulose extract. There is difference between the pyrolysis of *P. G.* peel and cellulose extract

The determination coefficients corresponding to the linear fittings and the resultant activation energy values calculated by the Popescu, FWO and KAS methods are shown in Table 4. The Popescu method did not adopt the temperature integral function and avoided the adaptability of Arrhenius equation and compensation effect problems. Therefore, the mechanism function determined by Popescu method is credible. The FWO and KAS methods are adopted to certify the results calculated by the Popescu method. *A* plot of $\ln\beta$, $\ln(\beta/T^2)$ versus $1/T$ gave straight lines with slopes of 1.0516 E/RT and E/R by the FWO and KAS methods. These methods have the advantage that they do not require a previous knowledge of the reaction mechanism to determine the activation energy.

The results in Table 4 indicate that the activation energy and $\ln A$ are very close and have confidence values ranging from 0.9284 to 1. Therefore, the activation energy calculated by the Popescu, FWO and KAS methods is valid. However, the activation energy increases fluctuation at different conversion rates. This may be ascribed to the complex composition of the samples and the complex reactions during pyrolysis. Among the two samples, the average activation energy of *P. G.* peel is the lowest. In every case, the relationship between the activation energy and pre-exponential factor was linear. In the literatures (Li et al., 2012; Bojan, 2014), this situation is called as kinetic compensation effect which arises from the kinetic models variation under the heating rate value changes, and defined as a rise in E (which will decrease the rate of reaction at any particular temperature) is partially or completely offset by an increase in A.

Table 5
Effects of pre-exponential factors on the activation energy.

Sample	Method	Equation	r
P. G. peel	FWO	$\ln A = 0.212E - 1.145$	0.9995
	KAS	$\ln A = 0.216E - 1.781$	0.9990
	Popescu	$\ln A = 0.215E - 1.480$	0.9995
Cellulose Extract	FWO	$\ln A = 0.231E + 8.783$	0.7239
	KAS	$\ln A = 0.236E + 7.678$	0.7457
	Popescu	$\ln A = 0.245E + 3.608$	0.8866

Table 5 indicates that there is a partial compensation for A when E changes. The R values of equations for *P. G.* peel with different methods are higher than those of equation for cellulose extract. Table 5 shows the $\ln A - E$ equation for each individual kinetic model included in the review, without effecting any change in the heating rate. These are consistent with the references that a kinetic

Table 6
Comparison of kinetic parameter of pyrolysis for different biomass.

Samples	Temperature (°C)	E (kJ/mol)	References
Wheat straw	230–400	130–175	He et al. (2002)
Cellulose in cotton	375	178 (Vyazovkin)	Matheus et al. (2010)
Walnut shell	175–351	76.3 (Horowitz)	Korkut (2011)
Eucalyptus BSP	270–440	190 (Coats), 190 (FWO)	Cornelia et al. (2011)
Abalone polysaccharide	282	29.5	Wang, He, and Kong (2009)
Ilex holly leaf polysaccharide	286	28.7	She, Hu, and Guo (2003)
Heparin	267	22.5	She et al. (2003)
Starch	309	17.1	She et al. (2003)
Pinus taeda	210–400	153–163 (FWO)	Luis and Noureddine (2010)

compensation effect existing in the pyrolysis of various biomass materials such that there is a definite linear correlation between the variables $\ln A$ and E (Bojan, 2014; John, Catallo, & Benjamin, 2011). According to the kinetic compensation effect, any alteration in experimental conditions that impels E to change will also prompt a complementary compensating response $\ln A$. A group of reactions that demonstrates a linear fit of $\ln A$ and E values is known as compensation set. It is claimed that reactions within a given compensation set exhibit unique properties, including shared chemical characteristics and the existence of an isokinetic temperature, T_i, at which all reactions advance at the same rate, k_i.

In Table 6, the comparison of various kinetic parameters of pyrolysis between different biomass sources is made. None of these published results are similar to the results in this paper, which suggests that thermal behavior is greatly influenced by the type of feedstock. This is because, according to the literatures (Wang et al., 2013; Wong et al., 2004), there are different components in different feedstock which has different pyrolytic characteristic.

4. Conclusion

(1) There are three stages in the pyrolytic process of the samples. Stage I involves the loss of cellular water, and the external water bound by surface tension; Stage II involves devolatilization; and during Stage III, the residue slowly decomposes, forming a loose porous residue. Heating rate has a significant effect on the pyrolysis of the three samples.

(2) The Popescu, FWO and KAS methods are adopted to determine the kinetic parameters of the reaction. During the primary decomposition reactions, the two samples exhibit different reaction mechanism. The function Avrami–Erofeev $[-\ln(1-\alpha)]^3$ is predominant during the main pyrolysis of *P. G.* peel. However, the function Chemical reaction $(1-\alpha)^{-0.5}$ is predominant during the main pyrolysis of cellulose extract. The activation energy calculated with these three methods is similar. The results of our study provide useful information for designing a pyrolytic processing system using biomass, especially *P. G.* peel, as feedstock. Pyrolytic reaction of cellulose extract occurs more easily than that of *P. G.* peel.

Acknowledgements

This work is financed by grants from Scientific Research Foundation for Returned Scholars, Ministry of Education of China, and China Postdoctoral Science Foundation National (Grant no. 1302006A).

References

Bojan, J. (2014). The pyrolysis of coffee paper cup waste samples using non-isothermal thermo-analytical techniques. The use of combined kinetic and statistical analysis in the interpretation of mechanistic features of the process. *Energy Conversion and Management*, *85*, 33–49.

Brebu, M., & Vasile, C. (2010). Thermal degradation of lignin. *Cellulose Chemistry and Technology*, *44*, 353.

Cai, J. M., & Bi, L. S. (2009). Kinetic analysis of wheat straw pyrolysis using isoconversional methods. *Journal Thermal Analysis Calorimetry*, *98*, 325–330.

Cornelia, V., Carmen, A. M., Popescu, M. C., Brebu, M. H., & Stefan, W. (2011). Thermal behavior/treatment of some vegetable residues. IV. Thermal decomposition of eucalyptus wood. *Cellulose Chemistry and Technology*, *45*, 29–42.

Dorez, G., Ferry, L., Sonnier, R., Taguet, A., & Lopez-Cuesta, J. M. (2014). Effect of cellulose, hemicellulose and lignin contents on pyrolysis and combustion of natural fibers. *Journal of Analytical and Applied Pyrolysis*, *107*, 323–331.

Hajaligol, M., Waymack, B., & Kellogg, D. (2001). Low temperature formation of aromatic hydrocarbon from pyrolysis of cellulosic materials. *Fuel*, *80*, 1799–1807.

He, F., Yi, W. M., & Sun, R. F. (2002). Pyrolys is and its kinetics of corn stalk and wheat straw. *Transactions of the CSAE*, *18*, 10–13.

He, Z. D., Qiao, C. F., Han, Q. B., Wang, Y., Ye, W. C., & Xu, H. X. (2005). New triterpenoid saponins from the roots of *Platycodon grandiflorum*. *Tetrahedron*, *61*, 2211–2215.

Hossain, M. K., Dewan, M. W., Hosur, M., & Jeelani, S. (2011). Effect of surface treatment and nanoclay on thermal and mechanical performances of jute fabric/biopolgreen'composites. *Journal of Reinforced Plastics and Composites*, *30*, 1841–1856.

Hu, R. Z., Gao, S. L., Zhao, F. Q., Shi, Q. Z., Zhang, T. L., & Zhang, J. J. (2008). (2nd ed., pp. 151). *Thermal analysis kinetics* (245–247) Beijing: Science Press [in Chinese]

Jeguirim, M., & Trouvé, G. (2009). Pyrolysis characteristics and kinetics of *Arundo donax* using thermogravimetric analysis. *Bioresource Technology*, *100*, 4026–4031.

John, E. W., Catallo, J. W., & Benjamin, L. L. (2011). Biomass pyrolysis kinetics: A comparative critical review with relevant agricultural residue case studies. *Journal of Analytical and Applied Pyrolysis*, *91*, 1–33.

Jones, J. M., Darvella, L. I., Bridgemana, T. G., Pourkashaniana, M., & Wliamsa, A. (2007). An investigation of the thermal and catalytic behavior of potassium in biomass combustion. *Proceeding of the Combustion Institute*, *31*, 1955–1963.

Korkut, A. (2011). Thermo gravimetric analysis of walnut shell as pyrolysis feedstock. *Journal of Thermal Analysis and Calorimetry*, *105*, 145–150.

Lédé, J. (2012). Cellulose pyrolysis kinetics: An historical review on the existence and role of intermediate active cellulose. *Journal of Analytical and Applied Pyrolysis*, *94*, 17–32.

Li, D. M., Chen, L. M., Zhao, J. S., Zhang, X. W., Wang, Q. Y., & Wang, H. X. (2010). Evaluation of the pyrolytic and kinetic characteristics of *Enteromorpha prolifera* as a source of renewable bio-fuel from the Yellow Sea of China. *Chemical Engineering Research and Design*, *88*, 647–652.

Li, D. M., Chen, L. M., Zhang, X. W., Ye, N. H., & Xing, F. G. (2011). Pyrolytic characteristics and kinetic studies of three kinds of red algae. *Biomass and Bioenergy*, *35*, 1765–1772.

Li, D. M., Chen, L. M., Zhao Chen, S. L., Zhang, X. W., Chen, F. J., & Ye, N. H. (2012). Comparative evaluation of the pyrolytic and kinetic characteristics of a macroalga (*Sargassum thunbergii*) and a freshwater plant (*Potamogeton crispus*). *Fuel*, *96*, 185L 191.

Luis, C., & Noureddine, A. (2010). On the thermal degradation of cellulose in cotton fibers. *Journal Thermal Analysis Calorimetry*, *102*, 485–491.

Maheswari, C. U., Obi Reddy, K., Muzenda, E., Guduri, B. R., & Varada, R. A. (2012). Extraction and characterization of cellulose microfibrils from agricultural residue e *Cocos nucifera* L. *Biomass and Bioenergy*, *46*, 555–563.

Matheus, P., Juliane, D., Vinícios, P., Mara, Z., & Ademir, J. Z. (2010). Materials produced from plant biomass Part I: Evaluation of thermal stability and pyrolysis of wood. *Materials Research*, *13*, 375–379.

Matsuoka, S., Kawamoto, H., & Saka, S. (2014). What is active cellulose in pyrolysis? An approach based on reactivity of cellulose reducing end. *Journal of Analytical and Applied Pyrolysis*, *106*, 138–146.

Mohammad, K. H., Mohammad, R. Karim, Mahmudur, R. C., Muhammad, A. I., Mahesh, H., Shaik, J., & Ramsis, F. (2014). Comparative mechanical and thermal study of chemically treated and untreated single sugarcane fiber bundle. *Industrial Crops and Products*, *58*, 78–90.

Park, Y. H., Kim, J., Kim, S. S., & Park, Y. K. (2009). Pyrolysis characteristics and kinetics of oak trees using thermo gravimetric analyzer and micro-tubing reactor. *Bioresource Technology*, *100*, 400–405.

Raveendran, K., Ganesh, A., & Khilar, K. C. (1996). Pyrolysis characteristics of biomass and biomass components. *Fuel*, *75*, 987–998.

Rupérez, P. (2002). Mineral content of edible marine seaweeds. *Food Chemistry*, *79*, 23–26.

Shaik, S. M., Sharratt, P. N., & Tan, R. B. H. (2013). Influence of selected mineral acids and alkalis on cellulose pyrolysis pathways and anhydrosaccharide formation. *Journal of Analytical and Applied Pyrolysis*, *104*, 234–242.

She, Z. G., Hu, G. P., & Guo, Z. Y. (2003). Study on the Thermal decomposition of the sulphated polysaccharide Hal-A from haliotis diversicolor Reeve. *Chinese Journal of Organic Chemistry*, *23*, 1149–1151 (in Chinese).

Van de Velde, K., & Baetens, E. (2001). Thermal and mechanical properties of flax fibres as potential composite reinforcement. *Macromolecular Materials and Engineering*, *286*, 342–349.

Wang, X., He, L. L., & Kong, Y. M. (2009). A study on thermal analysis of broadleaf holly leaf and Chinese ilex leaf polysaccharide KPS IIIa. *Food Science*, *44*, 44–46 (in Chinese).

Wang, S., Ru, B., Lin, H., & Luo, Z. (2013). Degradation mechanism of monosaccharides and xylan under pyrolytic conditions with theoretic modeling on the energy profiles. *Bioresource Technology*, *143*, 378–383.

Wei, X. L., Wang, Z., Wu, Y., Yu, Z. M., Jin, J., & Wu, K. (2014). Fast pyrolysis of cellulose with solid acid catalysts for levoglucosenone. *Journal of Analytical and Applied Pyrolysis*, *107*, 150–154.

Wong, S., Shanks, R., & Hodzic, A. (2004). Interfacial improvements in poly (3-hydroxybutyrate)-flax fibre composites with hydrogen bonding additives. *Composites Science and Technology*, *64*, 1321–1330.

Zhou, Q. C. (2011). Microwave-assisted extraction for isolating platycodin from *Platycodon radix*. *International Agricultural Engineering*, *20*, 124–129.